

## Angle-Resolved Photoemission from Surface States

E. E. Krasovskii<sup>1</sup> and W. Schattke<sup>1,2</sup>

<sup>1</sup>*Institut für Theoretische Physik, Christian-Albrechts-Universität, Leibnizstrasse 15, D-24098 Kiel, Germany*

<sup>2</sup>*Donostia International Physics Center, P. Manuel de Lardizábal, 4, 20018 Donostia-San Sebastián, Spain*

(Received 17 June 2003; published 7 July 2004)

The role of the evanescent part of the unoccupied complex band structure in photoemission from surface states is revealed. The frequency dependence of the emission intensity from two surface states on the (100) and (111) surfaces of Al in the photon energy range from 40 to 110 eV is explained within an *ab initio* one-step theory of photoemission. A novel embedding method to determine surface states is presented. A high sensitivity of surface states spectra to details of the surface potential barrier is predicted, which offers a way to efficiently monitor surface properties.

DOI: 10.1103/PhysRevLett.93.027601

PACS numbers: 79.60.-i, 71.15.-m, 73.20.-r

Spectroscopic measurements on surface states are a valuable source of information about various surface phenomena, such as surface magnetization, reconstruction, or adsorption [1]. The majority of measurements have, however, concentrated on monitoring the surface state energy ( $\mathbf{k}^{\parallel}$  dispersion), and little attention has been paid to wave functions. The interpretation of the frequency dependence of the emission intensity has been limited to the spectral decomposition theory of Louie *et al.* [2], which assumes a nearly free-electron (NFE) dispersion of final states [2,3]. The complex band structure (CBS) in the final states region is, thus, completely ignored and the width of the “emission window” is explained by the spatial localization of the initial state ( $k^{\perp}$  broadening) plus the broadening due to inelastic processes. The understanding of angle resolved photoemission (PE) depends upon accurate *ab initio* calculations of the spectra: a simplified treatment of the final states by intuitive arguments of spectral density or band mapping may be totally misleading [4]. The aim of the present paper is to go beyond the propagating-states-only approach and develop a picture of photoemission from surface states based on the one-step photoemission theory [5]. We shall reveal a rich non-NFE structure of high-energy states and show how it is reflected in constant-initial-state spectra.

We shall consider delocalized surface states, that slowly decay into the bulk, and we shall find the spectra to be very sensitive to the bulk asymptotics of the wave function. This calls for an *ab initio* technique that would treat accurately both the crystal-vacuum interface and the bulk half space. With this aim we propose an *embedding method*, in which the substrate is represented by its complex band structure, i.e., by a set of solutions of the bulk Schrödinger equation, which, for a given energy  $E$  and a surface projection  $\mathbf{k}^{\parallel}$  of the Bloch vector, are characterized by their normal projections  $k^{\perp}$ :  $\hat{H}_{\text{bulk}}\psi^{\text{B}}(E, \mathbf{k}^{\parallel} + \mathbf{n}k^{\perp}; \mathbf{r}) = E\psi^{\text{B}}(E, \mathbf{k}^{\parallel} + \mathbf{n}k^{\perp}; \mathbf{r})$ . Intrinsic surface states occur in the gaps of a  $\mathbf{k}^{\parallel}$  projected real band structure, i.e., at the energies at which there are no solutions with

purely real  $k^{\perp}$ . The wave functions  $\psi^{\text{B}}$  are obtained with the inverse extended linear augmented plane waves  $\mathbf{k} \cdot \mathbf{p}$  method (ELAPW) [6].

The embedding setup for the Al(100) surface is shown in Fig. 1. The substrate occupies the half space  $z < z_{\text{M}}$ ; it is described by a periodic bulk potential  $V_{\text{bulk}}$ . To describe the surface region, we introduce a slab, which is confined between  $z_{\text{L}}$  and  $z_{\text{V}}$  and contains nine atomic layers and a vacuum region. The slab potential  $V_{\text{slab}}$  gradually deviates from the bulk distribution and matches the constant vacuum value at  $z = z_{\text{V}}$ . The slab is repeated to form a crystal for which a band structure problem is solved and a self-consistent potential  $V_{\text{slab}}$  is obtained. The embedded region  $\Omega$ ,  $[z_{\text{M}}, z_{\text{V}}]$ , is a fragment of the slab. The matching plane  $z = z_{\text{M}}$  is placed deep enough in the slab, so that the potential near  $z_{\text{M}}$  matches the bulk potential. By embedding we mean the continuation of a substrate Bloch wave

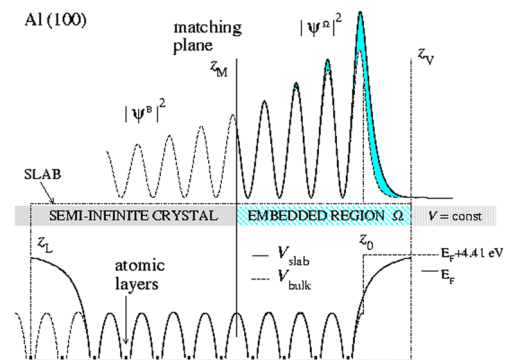


FIG. 1 (color online). Plane-averaged density distribution in surface state on Al(100) surface at  $\bar{\Gamma}$ . An evanescent bulk solution  $\psi^{\text{B}}$  (dashed line) is continued into surface region with initial conditions defined at  $z_{\text{M}}$ . Full line is density by embedding method. For  $z > z_0$ , dashed line is a continuation of  $\psi^{\text{B}}$  into vacuum: assuming an abrupt change of bulk potential to a constant at  $z = z_0$ , function is matched to a vacuum solution only in value. Lower panel: crystal potential in embedding method: for  $z < z_{\text{M}}$  it is a self-consistent bulk potential; for  $z_{\text{M}} < z < z_{\text{V}}$  it is a self-consistent potential of repeated slab.

$\psi^B$  to the interface region  $\Omega$ . Given the initial conditions at the plane  $z = z_M$ ,

$$\psi^\Omega(\mathbf{r}^\parallel, z_M) = \psi^B(\mathbf{r}^\parallel, z_M), \quad (1)$$

$$\partial_z \psi^\Omega(\mathbf{r}^\parallel, z_M) = \partial_z \psi^B(\mathbf{r}^\parallel, z_M), \quad (2)$$

we integrate the Schrödinger equation over the embedded region. We denote by  $\{\xi_m\}$  the set of slab eigenfunctions at the point  $\Gamma$ :  $\hat{H}_{\text{slab}} \xi_m = \epsilon_m \xi_m$ . Any function periodic in the interval  $[z_L, z_V]$  can be expanded in a convergent series in terms of  $\xi_m$ . Obviously, in the region  $\Omega$ , the continuation of the function  $\psi^B$  can be represented by a series of the slab solutions with any desired accuracy:  $\psi^\Omega = \sum_m a_m \xi_m$ . A novel aspect of our method is that instead of solving the equation  $(\hat{H}^\Omega - E)\psi^\Omega = 0$  we solve an equivalent equation  $\gamma(\hat{H}^\Omega - E)\psi^\Omega = 0$ , where  $\gamma(\mathbf{r})$  is a positive definite function. We find the coefficients  $a_m$  by minimizing the energy deviation  $\Delta E = \|\gamma(\hat{H}^\Omega - E)\psi^\Omega\|$ ,

$$\Delta E = \sum_{m'm} (\epsilon_{m'} - E)(\epsilon_m - E) \omega_{m'm} a_{m'}^* a_m, \quad (3)$$

under the constraints (1) and (2). Computationally, the problem reduces to calculating the overlap integrals

$$\omega_{m'm} = \int_{\Omega} \gamma(\mathbf{r}) \xi_{m'}^*(\mathbf{r}) \gamma(\mathbf{r}) \xi_m(\mathbf{r}) d^3r. \quad (4)$$

The function  $\gamma(\mathbf{r})$  is chosen such that the functions  $\gamma(\mathbf{r}) \xi_m(\mathbf{r})$  have a rapidly convergent plane-wave expansion [7]. The performance of the method depends upon (i) the quality of the functions  $\xi_m$  [Eq. (3) assumes that they pointwise satisfy the Schrödinger equation]; (ii) the quality of the PW expansion, which determines the accuracy of the integrals (4). In the LAPW method both requirements have proved to be easily fulfilled, which gives rise to an efficient plane-wave formulation of the embedding problem without resorting to pseudopotentials.

The determination of the surface state proceeds as follows: since the plane  $z = z_M$  lies far from the surface the surface state for  $z < z_M$  can be represented by a single evanescent wave  $\psi^B(\mathbf{r})$ , which delivers the boundary constraint (1) on the value of  $\psi^\Omega(\mathbf{r})$  at  $z_M$  (the slope being free). The second boundary condition is given by the exponential decay of the function at  $z \rightarrow +\infty$ . For a given energy  $E$ , the solution of the boundary value problem is unique. It is obtained by solving the variational equation  $\delta \|\gamma(\hat{H}^\Omega - E)\psi^\Omega\| = 0$  under the given boundary constraints [13]. Then, the energy is sought at which the function turns out smooth at  $z = z_M$ , i.e., the derivative condition (2) is satisfied. The advantage of this method over previously used schemes [8] is that it employs a self-consistent non-muffin-tin all-electron potential over the whole space and uses a semi-infinite crystal geometry, which ensures a correct evanescent asymptotics of the wave functions both in the vacuum and in the bulk.

In the experiment of Ref. [9], the surface state on the Al(100) surface at  $\mathbf{k}^\parallel = 0$  is located at 2.75 eV below the Fermi level in a gap between the  $X'_4$  (2.83 eV) and  $X_1$  (1.15 eV) states. Recent measurements of Ref. [10] locate the surface state at 2.5 eV. Our calculation yields 2.78 and 1.78 eV for  $X'_4$  and  $X_1$ , respectively, and  $E_{ss}^{100} = 2.62$  eV for the surface state. In the bulk, the surface state is a single evanescent wave with the real part of the Bloch vector  $k_{ss}^\perp$  at point  $X$  and an imaginary part of  $0.036 \text{ \AA}^{-1}$ . A contribution from the steeply decaying waves at the surface gives rise to the shaded area to the left from  $z_0$  in Fig. 1. The Al(111) surface state is experimentally observed at 4.56 eV below the Fermi level [3], and in our calculation it is at  $E_{ss}^{111} = 4.47$  eV. It is located in a narrow 0.25 eV wide gap at the point  $L$  and decays much slower into the bulk:  $\text{Im } k_{ss}^{111} = 0.013 \text{ \AA}^{-1}$ .

The (100) surface state is very sensitive to the shape of the potential in the vicinity of the surface; for example, with a steplike potential (see Fig. 1) it occurs at  $E_{ss}^{100} = 2.32$  eV with  $\text{Im } k_{ss}^{100} = 0.045 \text{ \AA}^{-1}$ . Because of the very narrow gap at the point  $L$  the effect of the potential on the (111) surface state is an order of magnitude smaller.

In the *one-step theory* [5], the PE intensity is determined by the probability of the optical transition from the initial state  $|ss\rangle$  to a time-reversed low energy electron diffraction (LEED) state  $|\text{LEED}^*(\mathbf{k}^\parallel, E_{\text{fin}})\rangle$ . We ignore the local field effects near the surface, so the perturbation operator reduces to  $-i\nabla$ :

$$J(E) \sim \sqrt{E - E_{\text{vac}}} |\langle \text{LEED}^*(E) | -i\mathbf{e} \cdot \nabla | ss \rangle|^2. \quad (5)$$

We calculate the LEED states from the  $\mathbf{k}^\parallel$ -projected CBS using a variational matching approach described in Ref. [11]. Inside the crystal the LEED function is a sum of propagating and evanescent waves,  $\Phi = \sum_n \psi_n^B$ . The functions  $\psi_n^B$  are thought to include the matching coefficients. The finite escape depth of the photoelectron was taken into account by adding an imaginary term, the optical potential  $-iV_i$ , to the potential in the crystal half space. Optical potential describes the inelastic scattering according to the theory of Slater [12], and it is the only parameter of the calculation that we cannot determine from first principles. To compare our spectra with the experiment we use a realistic value of  $V_i = 2$  eV. To emphasize the structure of the curves in Fig. 2(d) and 3 we use a negligible value of  $V_i = 0.25$  eV.

Figure 2 presents our *ab initio* spectra for the surface state at the (100) surface of Al for  $k^\parallel = 0$  [ $\bar{\Gamma}$  in the first surface Brillouin zone (SBZ)] and for  $k^\parallel = 1.16$  a.u. ( $\bar{\Gamma}$  in the second SBZ). The present theory reproduces well the width and gross features of the measured spectra [9], in particular, the asymmetric shape of the  $\bar{\Gamma}(1)$  curve and the minimum at 70 eV in the  $\bar{\Gamma}(2)$  spectrum. The latter is a compelling evidence of the inadequacy of the NFE model at high energies, which would lead to a Lorentzian-shaped curve [2,3]. We observe a rigid energy shift  $E_{\text{fin}} \rightarrow E_{\text{fin}} + 3$  eV of all experimental structures with respect to their calculated counterparts, which we ascribe to the

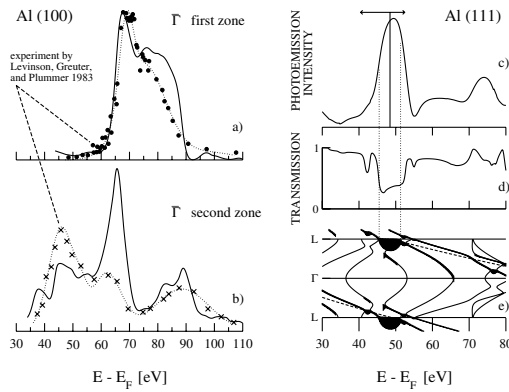


FIG. 2. Frequency dependence of PE intensity from surface state on Al(100) surface, (a) and (b), and on Al(111) surface, (c). Calculated spectra (full lines) are obtained with  $V_i = 2$  eV. Measured  $\bar{\Gamma}(1)$  spectrum [9] is shown by circles and  $\bar{\Gamma}(2)$  spectrum by crosses. (From Fig. 11 in Ref. [9].) To facilitate comparison, all our theoretical curves are shifted by 3 eV to higher energies. Horizontal arrow in graph (c) shows interval over which (111) state was observed in Ref. [3], and vertical line experimental location of intensity maximum. Graph (d) shows  $\mathbf{k}^{\parallel} = 0$  electron transmission spectrum  $T(E)$  for  $V_i = 0.25$  eV. Graph (e) compares real band structure along  $\Gamma L$  line (full lines) with NFE model of Ref. [3] (dashed lines). Only bands that determine LEED states are shown. Vertical extent of shaded area shows imaginary part of  $k^{\perp}$  for most important LEED constituents for  $V_i = 0.25$  eV.

simplified self-energy operator we have used: the exchange-correlation potential in the local density approximation. Our assumption is supported by the fact that all three spectra studied consistently exhibit the shift of about 3 eV. Our neglect of the local fields is expected to affect the  $\bar{\Gamma}(2)$  spectrum more strongly than the  $\bar{\Gamma}(1)$  spectrum, which may be the reason for the less favorable comparison to the experiment in the  $\bar{\Gamma}(2)$  case.

The wide emission interval is a consequence of the localized nature of the surface state, which levels out the  $k^{\perp}$  dependence of the transition probability and gives rise to an appreciable contribution from the evanescent part of

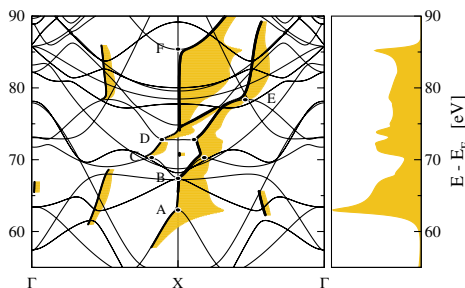


FIG. 3 (color online). Real band structure of Al along the  $\Gamma X \Gamma$  line (thin lines). Thick lines mark LEED constituents responsible for PE. Letters denote special points of real band structure. Horizontal extent of shaded bands shows modulus of matrix element (not squared) in Eq. (5). Data are obtained with  $V_i = 0.25$  eV; resulting  $\bar{\Gamma}(1)$ -PE spectrum is shown in right panel.

the unoccupied CBS. Since the real part of  $k_{ss}^{\perp}$  is at  $X$  and the imaginary part is rather small,  $0.023 \cdot 2\pi/a$ , the resonance final states  $\psi_n^B$  are located in the vicinity of point  $X$ . Figure 3 shows the relevant fragment of the real band structure superimposed on the  $E(k_n^{\perp})$  lines (thick lines) that mark the most important Bloch constituents of the final states. Letters  $A$  to  $F$  denote maxima and minima of the  $E(k_n^{\perp})$  function for  $V_i = 0$ , at which real lines of the CBS originate. Individual contributions to the photocurrent are shown by the shaded area, whose horizontal extent is proportional to the matrix element  $|\langle \psi_n^B | -ie \cdot \nabla | ss \rangle|$ . An important result is that the emission over wide intervals  $AB$ ,  $CD$ , and  $EF$  is due to genuine evanescent states. The effect of  $V_i$  on propagating states is much stronger than on evanescent states; the spatial damping of the  $\psi^B$  waves caused by the absorbing potential is of the first order in  $V_i$  for the former and of the second order for the latter [14]. As a result, the damping of the final states has a minor and somewhat paradoxical effect on the total width of the emission window: with a negligible value of  $V_i = 0.25$  eV it is unexpectedly wide: 23 eV, see right panel of Fig. 3. The full width at half maximum *decreases* with increasing  $V_i$  because the contribution from propagating states at the edges of the emission interval (points  $A$  and  $F$ ) is reduced with respect to the band-gap emission in the middle of the interval.

The non-NFE nature of the final states suggests an explanation to the recent observation [10] of the surface sensitivity at high energies in photoemission from Al(100): Different final states may be responsible for the bulk and the surface state emission, and inelastic effects may differently affect them. Within the present theory the effect of thermal diffuse scattering should be included into the optical potential. Its increase with temperature would affect in the first place the propagating states and damp relevant spectral structures with respect to the surface state emission. Assuming an evanescent-state origin of the surface state emission also at higher energies, one may expect the surface state peak to be more stable towards a temperature increase than the bulk peaks.

The measurements on the Al(111) surface state [3], in accord with our theory, reveal a much sharper resonance than in the (100) case [at  $\hbar\omega = 53$  eV, the vertical line at  $E - E_F = 48.4$  eV in Fig. 2(c)]. As in the (100) case, our calculated maximum occurs some 3 eV lower in energy. The NFE model of Ref. [3] [dashed curve in Fig. 2(e)] suggests a different interpretation of the spectrum: to reproduce the peak width without including inelastic effects one would have to assume the decay length of the surface state to be  $10 \text{ \AA}$  (actual value is  $77 \text{ \AA}$ ). To resolve the contradiction, the authors introduced a photoelectron inverse lifetime of 4.5 eV. On the contrary, in our theory the peak originates from a band gap, and its width is not very sensitive to inelastic effects.

Because the PE final states are time reversed LEED states one can judge on their character by considering the

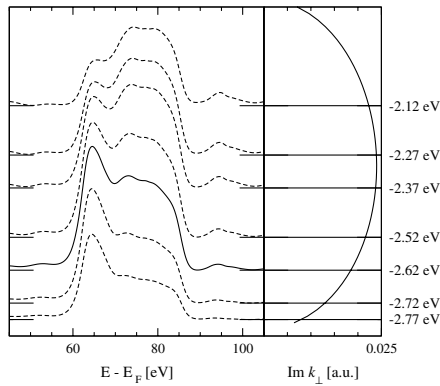


FIG. 4. Dependence of PE intensity distribution from Al(100) surface state on surface state energy (left panel). Spectrum for calculated surface state energy is shown by full line. Right panel shows real line of CBS for  $\text{Re } k_{\perp}$  at  $X$ .

energy dependence of the probability  $T(E)$  of the incident electron to be transmitted into the crystal. The normal incidence  $T(E)$  curve for the Al(111) surface is shown in Fig. 2(d). A deep 7 eV wide pit in the  $T(E)$  spectrum at the energy of the PE peak is another manifestation of the failure of the NFE model and of the dominant role of evanescent states.

The variations of the surface potential barrier lead to changes of the surface state energy [1]. However, for very slowly decaying states in narrow gaps of real band structure, the energy variations may be so small that they are difficult to detect experimentally and are comparable to uncertainties of theoretical approximations. At the same time, the changes in the wave function may be rather significant: for the Al(100) state, the energy shift by 0.3 eV from 2.62 to 2.32 eV results in a change of the state localization (expressed by  $\text{Im } k_{\perp}^{\perp}$ ) by 25% (see right panel of Fig. 4). Together with  $\text{Im } k_{\perp}^{\perp}$  changes the periodic part of the Bloch function, which is reflected in the frequency dependence of the emission intensity; left panel of Fig. 4. Figure 4 shows that the redistribution of the spectral intensity over the final states interval is very strong [15]: the location of the global maximum moves by 10 eV while the surface state energy changes by 0.3 eV. Such transformations are not only reliably resolved experimentally, but are also much larger than inevitable errors of theoretical models. Comparing different versions of the spectrum in Fig. 4 to the experiment in Fig. 2(a) suggests that the surface state—in particular the value of  $\text{Im } k_{\perp}^{\perp}$ —is accurately determined by the present embedding method. A similar but smaller effect we observe for the (111) surface: every shift of the surface state energy by 0.05 eV moves the maximum of the emission peak by 1 eV. Thus, we infer that the photoemission device may serve as a magnifying glass to monitor the effect of various processes on surface states.

To conclude, we have developed an *ab initio* theory of the surface states photoemission. A fundamental role of unoccupied evanescent states in the formation of the

spectra is established. The theory explains the location and the width of the surface state emission windows and reproduces the changes of these parameters from one experiment to another. The inelastic effects are shown to have a little effect on the width of the window. An explanation is offered for the surface sensitivity at high energies in photoemission from Al(100). The photon energy dependence of the emission cross section is found very sensitive to the bulk asymptotics of the surface state wave function. Small variations of the surface potential barrier can, thus, be monitored by measurements over a wide interval of final state energies, even though they cause only tiny changes of the surface state energy.

We acknowledge the support of Deutsche Forschungsgemeinschaft to E. E. K. (Forschergruppe FOR 353).

- [1] N. Memmel, Surf. Sci. Rep. **32**, 93 (1998).
- [2] S. G. Louie *et al.*, Phys. Rev. Lett. **44**, 549 (1980).
- [3] S. D. Kevan, N. G. Stoffel, and N. V. Smith, Phys. Rev. B **31**, 1788 (1985).
- [4] See the discussion of final states effects in PE from Bi2212: A. Bansil and M. Lindroos, Phys. Rev. Lett. **83**, 5154 (1999); H. M. Fretwell *et al.*, *ibid.* **84**, 4449 (2000).
- [5] P. J. Feibelman and D. E. Eastman, Phys. Rev. B **10**, 4932 (1974).
- [6] E. E. Krasovskii and W. Schattke, Phys. Rev. B **56**, 12874 (1997).
- [7] For the integrals (4), APWs are impractical because the matching plane intersects the muffin-tin spheres. An efficient PW expansion of the functions  $\gamma\xi_m$  is achieved by setting  $\gamma(\mathbf{r}) = 1$  everywhere except for spheres of radius  $r_{\gamma} = 1$  a.u. around the nuclei. The function  $\gamma(r)$  steadily diminishes from  $\gamma(r_{\gamma}) = 1$  to  $\gamma(0) = 0$ . See E. E. Krasovskii and W. Schattke, Phys. Rev. B **60**, 16251 (1999), and Ref. [17] therein.
- [8] E. Caruthers, L. Kleinman, and G. P. Alldredge, Phys. Rev. B **8**, 4570 (1973); D. Spanjaard, D. W. Jepsen, and P. M. Marcus, *ibid.* **19**, 642 (1979); E. Inglesfield and G. A. Benesh, *ibid.* **37**, 6682 (1988); E. V. Chulkov and V. M. Silkin, Surf. Sci. **215**, 358 (1989).
- [9] H. J. Levinson, F. Greuter, and E. W. Plummer, Phys. Rev. B **27**, 727 (1983).
- [10] Ph. Hofmann *et al.*, Phys. Rev. B **66**, 245422 (2002).
- [11] E. E. Krasovskii and W. Schattke, Phys. Rev. B **59**, 15609 (1999).
- [12] J. C. Slater, Phys. Rev. **51**, 840 (1937).
- [13] The variational ansatz for the half space of constant potential is described in Ref. [11].
- [14] See Eqs. (43) and (45) in Ref. [6].
- [15] The curves in Fig. 4 were not explicitly calculated for different surface potentials, but an energy scan was made over the gap by extrapolating the evanescent states to the vacuum with an “inaccurate” solution (dashed line for  $z > z_M$  in Fig. 1). This is justified for extended states because the dominant contribution to the matrix element comes from the bulk.